Journal of Building Engineering 44 (2021) 102642

Contents lists available at ScienceDirect

Journal of Building Engineering

journal homepage: http://www.elsevier.com/locate/jobe

The application of control algorithm for optimal performance of evaporatively-cooled façade system in hot dry and humid weathers

Albert Al Touma, Djamel Ouahrani *

Department of Architecture and Urban Planning, College of Engineering, Qatar University, P.O. Box 2713, Doha, Qatar

ARTICLE INFO

Keywords:
Control algorithm
Energy savings
Evaporatively-cooled façade
Heat gain
Thermal load

ABSTRACT

An evaporatively-cooled façade system, composed of a Photovoltaic thermal (PVT), evaporative cooler, and evaporatively-cooled façade, was previously developed. In this study, a control algorithm for the system parameters is implemented and applied on spaces with evaporatively-cooled façade to generate the least possible façade temperature, and consequently maximum possible energy savings. The optimization of the system parameters is expected to overcome the limitations of using evaporative coolers in humid countries. The application of the control algorithm managed to increase the reductions in the façade heat gain from 33.5% to 38.3%.

The system, integrated with the control algorithm, is then applied throughout the year on spaces located in Doha (Qatar) and Riyadh (Saudi Arabia), mimicking cities with harshly hot humid and dry weather conditions, respectively. The daily and monthly performances are further investigated in four different space orientations (i.e., north, east, south, and west). It was found that the application of the system can halve the highly glazed façade heat gain during the summer, in all orientations, and may have adverse, yet desirable effect during the winter. The integration of the control algorithm managed to reduce differences in system performance between dry and humid locations, thus generating total annual savings of up to 21.8% in any typical city of the Arabian Gulf.

1. Introduction

As more awareness is brought to the proliferating complications of both energy exhaustion and hazardous emissions, the growth rates in global annual energy consumption and carbon emissions have trended to less than 1% and 0.1% respectively, over the past three years [1]. According the BP Statistical Review of World Energy, however, many developing countries are problematically not contributing towards this international trend, especially those located in harshly hot weather climates of the Arabian Gulf, likely due to the abundant presence of energy resources [1].

Despite the widespread adoption of energy-reduction methods, residential and commercial buildings are still the primary energy-consuming sector in hot climates. In fact, these buildings consume 65% and 60% of the total electricity produced in the Kingdom of Saudi Arabia (KSA) and the State of Qatar, respectively [2,3]. By exceeding the world's average, this sector eventually formed the primary source of energy exhaustion in these countries [1]. In buildings, and among all components of the thermal envelope, glazed surfaces are still considered as the weakest; they transmit significant amounts of solar radiation, and absorb and re-emit large amounts, ultimately increasing the space energy demands significantly [4]. This problem has even magnified as the shift from small windows to fully glazed façades progressed, due to their numerous benefits on the building architecture, indoor daylighting, and occupant productivity [4,5]. Consequently, this progression has slowed these country's improvements towards energy conservation and their corresponding visions for a cleaner future [5].

Many researches have traditionally focused on glazed surfaces as means to reduce energy consumption in buildings. On one hand, these studies mitigated solar radiation transmission into spaces through the proper design of space orientation [6] and the appropriate selection of window optical properties using either normal glazing [7,8], near-infrared electrochromic glazing [9] or thermochromic glazing [10]. On the other hand, other studies found energy savings by reducing the glass solar absorption effect through the use of multiple-pane windows [11], airflow windows, double-skin façades [12–14], and the addition of phase-change materials to window cavities [15]. Moreover, simultaneous reductions in solar transmission and absorption were found through the addition of fixed or dynamic shading devices, such as shutters [4], solar films [16], brise soleil [17], and blinds [18,19]. Although

* Corresponding author.
E-mail address: djamel@qu.edu.qa (D. Ouahrani).

Available online 12 May 2021
https://doi.org/10.1016/j.jobe.2021.102642
2352-7102/
Received 9 January 2021; Received in revised form 1 April 2021; Accepted 28 April 2021

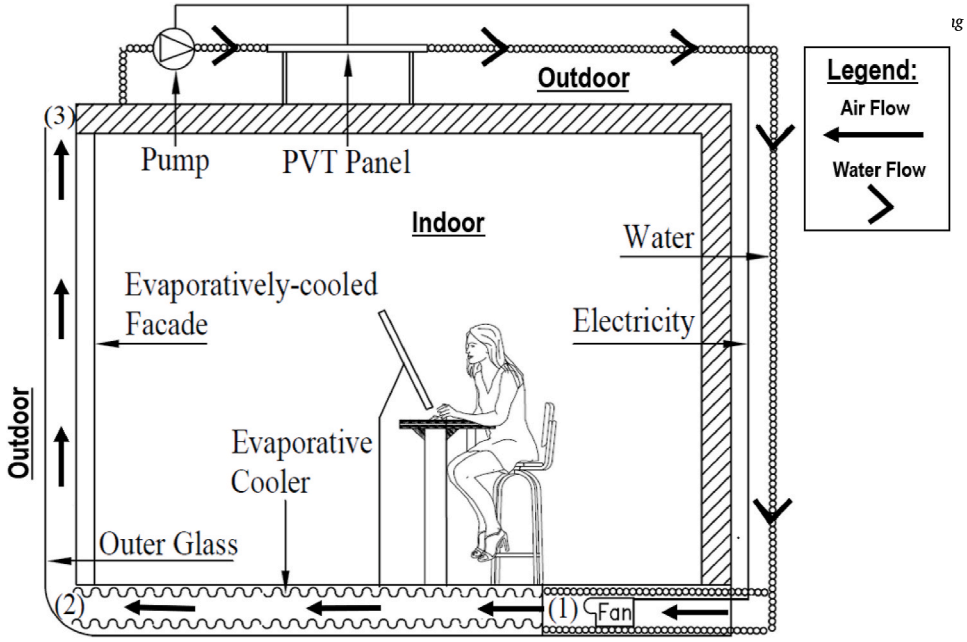

Fig. 1. Schematic of the evaporatively-cooled façade system applied on an office space.

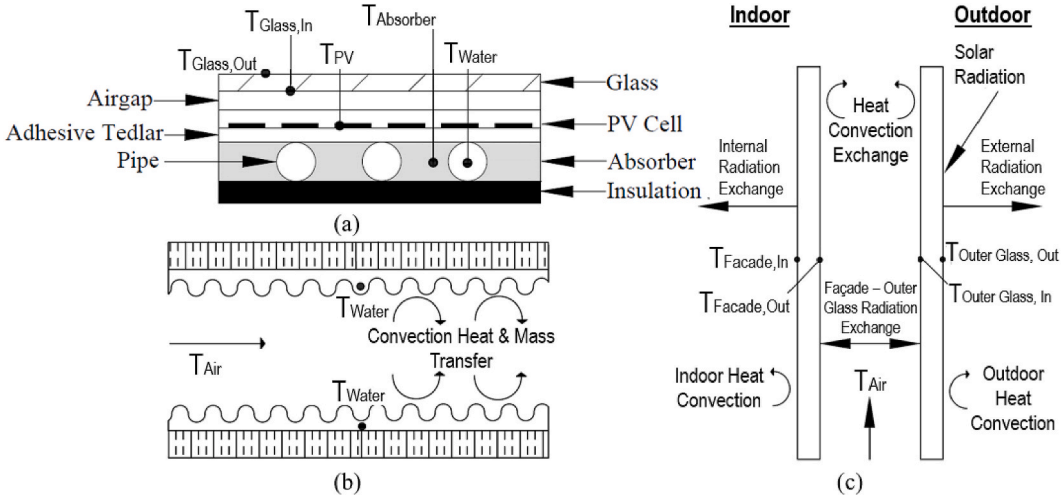

Fig. 2. Schematics representing the modeling of the (a) PVT panel, (b) Evaporative cooler and (c) Evaporatively-cooled façade [23].

all these methods managed to reduce the space energy demands in hot climates variably, the change in space orientation in unfeasible in existing buildings, the switch into high-performance glazing is very expensive to adopt, and the entrainment of outdoor air in airflow windows and façades performs poorly, or even adversely, in harshly hot climates. Moreover, the integration of shading devices, at least, causes partial obstruction of the outdoor visual sight, which is the primary purpose behind having fully-glazed façades. Hence, this sheds lights on the necessity to design novel and controlled passive cooling strategies that are freely driven by a renewable source of energy and are capable of reducing the glass temperature and space cooling energy demands, such as the evaporatively-cooled windows and evaporatively-cooled façades.

One of the successful passive cooling techniques is the system comprising of a solar chimney and a passive evaporative cooler applied on glazing surfaces, or the so-called evaporatively-cooled window [20]. In this system, the solar chimney and evaporative cooler are placed vertically above and below the window level respectively, and enclose the system using an outer glass layer. The solar radiation striking the chimney surface drives a natural upward buoyant flow in the entire system; outdoor air is cooled in the evaporative cooler, rendering it very capable at extracting heat from the window surface. The application of the evaporatively-cooled window during one summer representative day was found to save 19.8% of the space energy demands in the hot and dry climate of Riyadh (KSA), and 13.1% and 11.3% in the hot and humid climates of Jeddah (KSA) and Doha (Qatar), respectively [20,21]. Although the application of the system was found to save 8.8% of the space annual energy demand in Qatar [21] and enhance the human thermal comfort inside the space [22], its limited performance in humid climates as well as its applicability only to small window surfaces troubled its economic feasibility in some countries.

In a previous study conducted by the authors, the system of evaporatively-cooled façade integrated with Photovoltaic Thermal (PVT) panel was introduced and developed [23]. This system, which is driven by the solar energy striking a PVT surface rather than a solar chimney, powers a fan and a pump to forcefully entrain outdoor air and extract more heat from the façade surface. Furthermore, this system overcomes many design issues facing the application of the evaporatively-cooled window in humid climates [23]. Upon its successful modeling and ex-

Fig. 3. The evaporatively-cooled façade system installed in the Zero Emission laboratory for experimental validation.

Table 1
Model and experimental results of air at the outlets of the evaporative cooler and glazing section during two representative hours.

	Evaporative Cooler Outlet Air Temperature (°C)		Glazing Section Outlet Air Temperature (°C)	
	Simulation	Experiment	Simulation	Experiment
Time = 11 h (T_o = 43.8 °C, RH_o = 30%, Q_{ver} = 358 W/m^2, Q_{hor} = 964 W/m^2)	39.6	40.4 ± 0.5	42.4	44.5 ± 0.5
Time = 14 h (T_o = 40.7 °C, RH_o = 31%, Q_{ver} = 309 W/m^2, Q_{hor} = 863 W/m^2)	36.3	38.1 ± 0.5	39.2	42.3 ± 0.5

perimental validation, this system was found to save 33.5% and 14.5% of the façade total heat gain and space total energy demand during one representative day in the humid climate of Doha (Qatar) [23]. However, these energy savings are pertinent to one case study and may vary significantly depending on the weather conditions and façade orientation. More importantly, a control algorithm that manages the interactions between the system subcomponents has not been implemented. Due to the numerous heat transfer complexities inside the system, airflow controls are needed to intensify energy savings caused by its installation.

In this study, a control algorithm managing the interactions between all the subcomponents of the evaporatively-cooled façade system is proposed to optimize its performance in reducing the space energy demands. Then, the annual performance of the system is analyzed when applied on office spaces in four different orientations in both Riyadh (KSA) and Doha (Qatar), mimicking cities with harshly hot dry and humid weather conditions, respectively. These countries have two dominating seasons throughout the year: namely a hot summer from April to November and a moderate winter from December to March. Lastly, the benefits of the system during each season are assessed separately for one summer and one winter days. The three variables (i.e., system control algorithm, weather climate, and space façade orientation) have been selected for this study due to their significant resulting impact on the proposed system and its components, and consequently on the space thermal performance.

2. Methodology

2.1. Description of evaporatively-cooled façade driven by PVT panel

The system integrating the evaporatively-cooled façade with the PVT is schematically represented in Fig. 1. The evaporative cooler, made of 1 cm thick aluminum material of rectangular cross section, is located horizontally below the space level, and contains water absorbing sheets all over its inner surfaces. Adjacently, the evapoartively-cooled façade consists of the original glazed façade, and an outer glass layer installed in front of it and enclosed on the sides to allow vertical air motion only. Note that the outer glass layer installed in front of the façade has a very high visible transmissivity so that it does not jeopardize the visual sight of the indoor occupants, especially that its sole purpose is to direct air passage upwards. On the other hand, the PVT is located on the space rooftop and powers a fan and a pump; the first is used to supply outdoor air to the evaporative cooler whereas the latter is used to supply water to both the PVT and the evaporative cooler.

The system functions as follows [23]. Once solar radiation strikes the PVT surface, solar energy is converted into electricity and stored in its battery. This electricity drives the fan that entrains outdoor air into the evaporative cooler. The outdoor air (State 1 in Fig. 1), which is predominantly hot throughout the year in hot climates, is cooled in the evaporative cooler through sensible and latent heat exchanges with the water absorbing sheets. The cooled air (State 2) is then drawn inside the glazing section where it extracts significant heat from the façade hot surface, before getting exhausted back out to the outer environment (State 3). However, the cooling effect of the evaporative cooler is the resultant of water evaporation; hence, its performance comes at the expense of its need for continuous water supply. For this reason, the presumed need to cool the PVT surface with water is also used to meet the evaporative cooler demand. It is extremely important to mention that, based on its flow rate, the water cooling the PVT surface is heated by just few degrees above its original temperature, only to intensify the total cooling effect inside the evaporative cooler, both sensible and latent heat exchanges combined [23].

The system has three major characteristics. First, it provides cooling with minimal electrical requirements. In contrary to the direct usage of PVT-generated electricity for air-conditioning units, which requires large PVT surface areas, this system requires humble electrical needs just to power a small fan and pump. Second, this system forcefully drives airflow into the entire channel (i.e., evaporative cooler and then the glazed section). In comparison with the evaporatively-cooled window system that is naturally driven by a solar chimney, this system ensures much more cooling in the evaporative cooler and heat extraction in the glazing section using the concepts of forced rather than natural convection [20–22]. Third, this system overcomes the limited performance of the evaporative cooler in humid climates by placing it horizontally below, rather than vertically in front of, the space level. This physical design provides flexibility in selecting the length of the evaporative cooler so that, when both sensible and latent heat exchange occur, and despite minimal latent exchange when humidity of the circulating air is high, sensible exchange is intensified along the length of the cooler for maximum possible cooling.

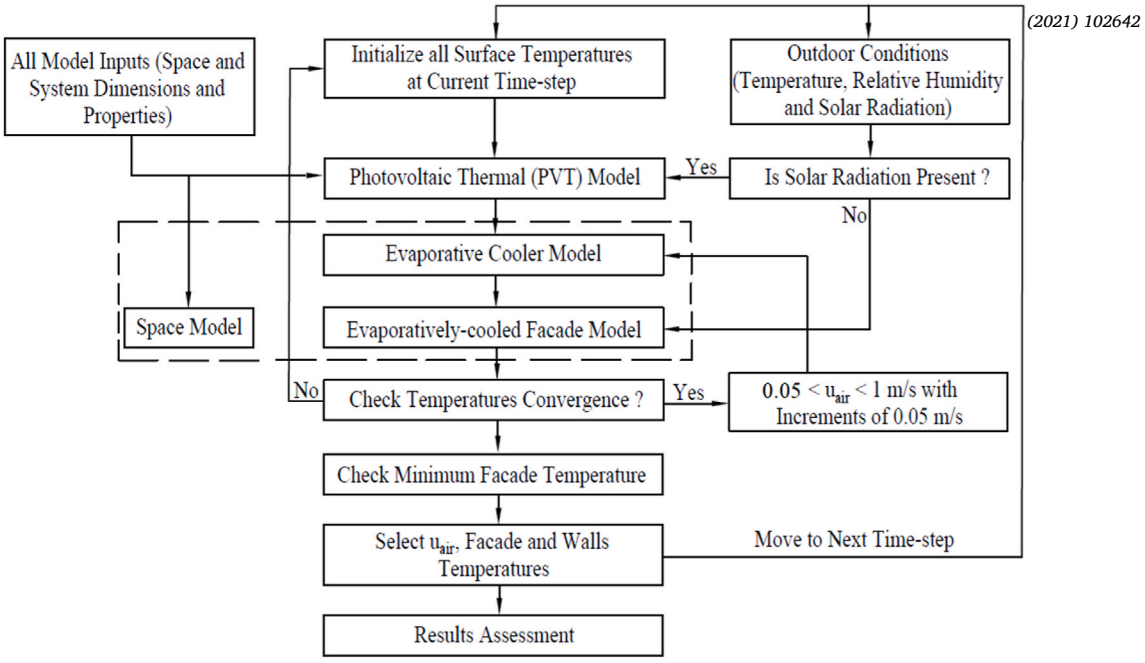

Fig. 4. Control algorithm for the evaporatively-cooled façade driven by PVT panel for optimal cooling performance.

2.2. System modeling

To study the performance of the system, a one-dimensional steady-state model was previously developed to describe the air property changes inside the channel along with the temperature variations of all the system subcomponents [23]. As the airflow in the system is powered by a fan, the air property changes assume forced convection in the evaporative cooler and glazing section, with negligible natural buoyant flow in the later. Fig. 2 shows schematics of the three main subcomponents of the system: PVT, evaporative cooler, and evaporatively-cooled façade. Note that the complete modeling details of each component is detailed in Ref. [23].

The PVT model of Herrando et al. [24] was adopted. As seen in Fig. 2(a), the PVT is composed of a glass layer, an airgap separating the glass from the PV modules, adhesive tedlar layer with an encapsulating film, an absorber with passing water pipes, and a back-insulation layer [23,24]. The developed energy balance equations consider radiation transmission and absorption through glass, radiation exchange between surfaces, convection of outdoor air with the glass and conduction through the different layers. Similarly, the energy exchange inside the water pipes balances the heat flux of the water with the convection heat transfer from the absorber to the water.

In the evaporative cooler, the model considers air heat and mass transfers separately [20,23,25]. As shown in Fig. 2(b), the mass balance equates the mass flux of the passing air with the convective moisture gain, whereas the heat equation balances the heat flux with both sensible and latent heat exchanges with the water sheets.

As for the evaporatively-cooled façade, the model divides this section into three main layers; outer glass, air, and façade layers, as schematically represented in Fig. 2(c). It takes the air temperature from the evaporative cooler as an input, and considers radiation absorption and transmission through glass, radiation exchange of glass with the sky, radiation exchange between the glass layers, conduction through the different layers, convection of outdoor air with glass, convection of entrained air with outer glass and façade, and radiation exchange between the façade and each of the space internal walls. Lastly, the fan and pump used in the system were assumed to supply constant flows with a predefined efficiency [23].

The convection heat transfer coefficient of outdoor air with glass was found using Hagisihma et al. [26] model based on the wind velocity. The radiation heat transfer coefficients between a surface and sky, or between surfaces, were found based on their temperature states, emissivities and their corresponding view factors [27,28]. In addition, the sky temperature was estimated using the outdoor dry-bulb temperature, dew-point temperature and hour time, based on the model developed by Duffie and Beckman [28]. Moreover, the heat and mass convection coefficients inside the evaporative cooler and glazing section were calculated using Gnielinski correlation for Nusselt number [29] and assuming a Lewis number of unity [20,25].

As the intended objective is the application of the system on an office space with fully-glazed façade in one pre-determined orientation, the space model of Yassine et al. [30] was adopted. This model, which distributes transmitted solar radiation over the space walls according to their surface areas, discretizes each surface in time and space to predict its hourly temperature at each discretized node using the implicit numerical scheme. The model also outputs the space hourly thermal load as well as the cumulative daily energy demand based on the inputted building thermal envelope, desired internal loads and selected outdoor conditions. All the mathematical equations used to model the integrated system and its components are detailed in Ref. [23].

2.3. System experimental validation

Actual experiments were conducted at the Zero Emission Laboratory at Qatar University to validate the developed numerical model. One space contained inside the laboratory, whose walls are fully insulated except for the glazed façade, was used to install the entire system as shown in Fig. 3. The space indoor environment was controlled as desired using a chiller with sensors that measured the chilled water inlet and exhaust conditions. Detailed description of the experimental setup and protocol are found in Ref. [23].

To better assess its ability in mimicking the space conditions, the model was validated under two cases for 24 consecutive hours; once without the system and once with the system installed on the façade external surface. The outdoor weather conditions were continuously measured at an adjacent meteorological site, averaged every hour, and then fed into the simulation model.

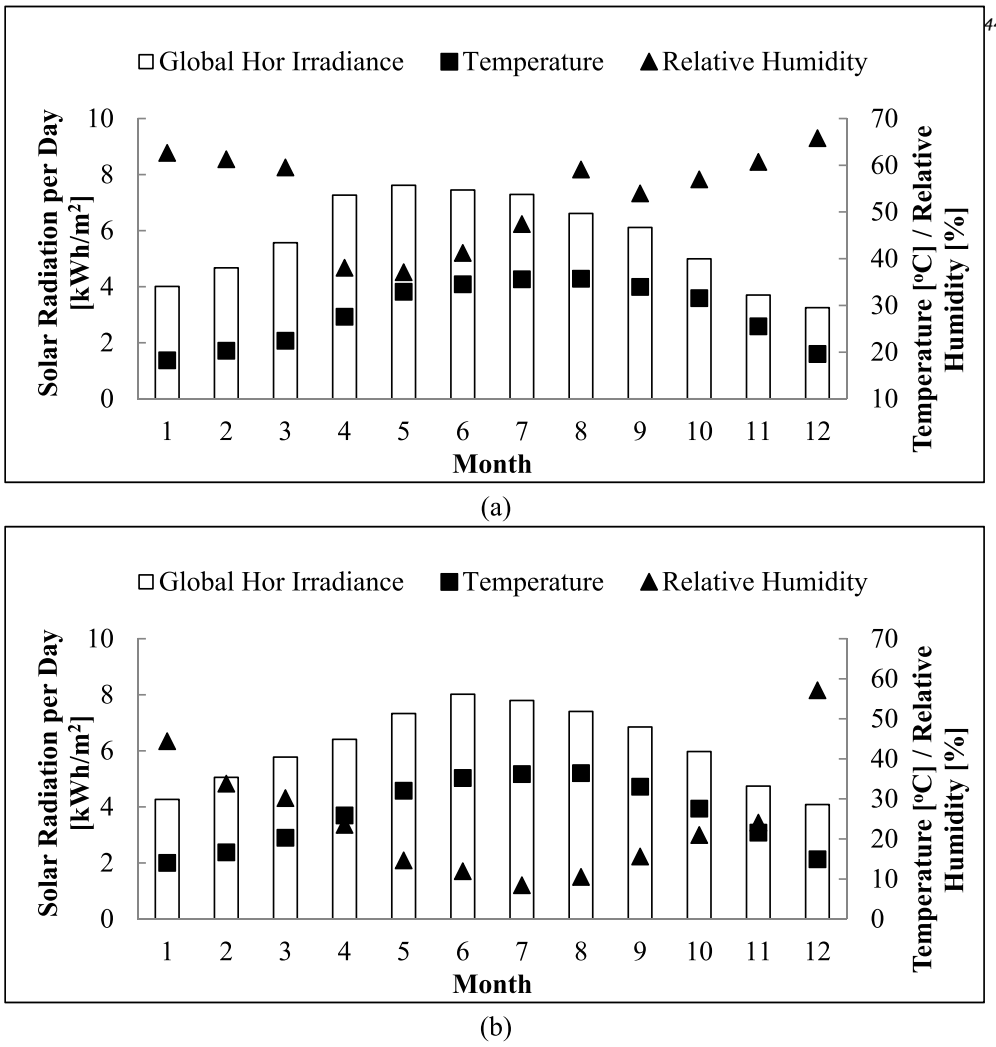

Fig. 5. Monthly averages of temperature, relative humidity, Global Horizontal Irradiance (GHI) for (a) Doha (Qatar) and (b) Riyadh (KSA).

Table 2
Technical specifications & material properties of the space envelope and evaporatively-cooled façade system [23,24,34,35].

Component	Properties
Façade	• Double-pane: 3 mm Clear – 6 mm airgap – 3 mm Clear (U-value = 3.23 W/m²·K) • SHGC = 0.76
Internal Walls	• 20 cm gypsum board
Floor & Ceiling	• 150 mm lightweight concrete (U-value = 3.8 W/m²·K)
Outer Glass	• 6 mm Clear glass (U-value = 6.31 W/m²·K) • SHGC = 0.9 • τ-*visible* = 0.88 • τ-*solar* = 0.77
Photovoltaic Thermal (PVT)	• Surface area = 1.56m² • Glass: t = 3 mm; ε = 0.84; τ = 0.9; α = 0.02; δ_d = 0.16; k = 0.0189 W/m·K; U-value = 6.31 W/m²·K; SHCG = 0.9 • Airgap: t = 5 mm; k = 0.026 W/m·K • Solar cells: PF = 0.9; α = 0.9; ε = 0.9 • EVA – adhesive tedlar: $U_{equivalent}$ = 500 W/m²·K • Absorber: α = 0.95; ε = 0.05 • Tubes: Diameter D = 1 cm; Number of Tubes N = 11 • Insulation: t = 2 cm; k = 0.02 W/m·K
Evaporative Cooler	• Aluminum of 1 cm thickness • Surface area = 6 m × 5 m • Gap = 5 cm

Table 3
Space internal loads accounted for in the case study.

Internal Load	Value
Two Occupants	130 W/person [36]
Two Computer Stations	200 W/computer [20]
Internal Lighting Load	1 W/ft² or 10.8 W/m² [37]

The validation process consisted of measuring the hourly values, for one whole day, of the air temperature at the evaporative cooler outlet and glazing section outlet (refer to states 2 & 3 in Fig. 1; measured at ±0.5 °C), the façade and outer glass inner and outer surface temperatures (at ±0.3 °C), and the space total thermal cooling load. The latter was calculated using the chilled water flow rate (at ±0.1 l/min) and inlet-outlet temperature difference (at ±0.1 °C) to maintain the indoor environment at 24 °C. For the case when the system was not installed (i.e., base-case office space), the maximum disparities, between the simulation and experiment, for the façade outer and inner surface temperatures were 0.8 °C ± 0.3 °C (2.9%) and 0.7 °C ± 0.3 °C (3.7%), respectively. The corresponding daily thermal energy demand was 1424 Wh in the simulation and 1463 ± 17 Wh in the experiment [23]. In the case when the system was installed, the maximum hourly disparities for the outer glass and façade outer and inner surface temperatures were 3.3 °C ± 0.3 °C (6.9%), 3.9 °C ± 0.3 °C (8.5%), 2.8 °C ± 0.3 °C (5.9%) and 1.6 °C ± 0.3 °C (6.0%). The space had a corresponding daily thermal energy demand of 1781 Wh in the model and

Table 4
Façade daily thermal heat gain with and without the integration of the control algorithm.

	Façade Daily Heat Gain (kWh)	Percentage Reduction (%)
Base-case Space	4.7	–
Space with System – No Control Algorithm	3.1	33.5
Space with System – With Control Algorithm	2.9	38.3

1732 ± 17 Wh in the experiment [23]. As for the air property changes inside the system (i.e., states 2 & 3 in Fig. 1), validation was carried out at all hours, two of which are illustrated in Table 1.

As shown in Table 1, good agreement was found between the predicted (i.e., model) and actual (i.e., experiment) air temperatures at the outlet of the evaporative cooler and glazing section. In summary, and for each two datasets, one representing the predicted temperatures through the model while the other representing the actual temperatures obtained through experimentation, strong correlation with statistical significance was found for both the façade and outer glass, exhibited by a maximum root mean square error (RMSE) of 1.5 °C and 0.4 °C with and without the system installed, respectively. Hence, it was concluded that the simulation model that integrates the evaporatively-cooled façade system with the space is actually valid. Note that the hourly performances of the façade and outer glass inner and outer surfaces, as well as that of the air inside the system (i.e., states 1, 2 & 3 in Fig. 1), used for temperature validation are all detailed in Ref. [23]. It is of interest to mention that the water passing through the PVT was numerically found to be heated by few degrees only (3–5 °C) and, as anticipated, was still capable of contributing towards both sensible and latent heat exchanges for maximum possible cooling in the evaporative cooler and optimal system performance.

The application of the system on a south-oriented office was found to save 33.5% and 14.5% of the façade daily heat gain and space total thermal energy demand respectively, during one summer representative day (July 21st) in Doha, Qatar [23]. The selected location represents a country with harshly hot and humid weather conditions. Despite the reductions in space loads, energy savings only correspond to the applied case study; outcomes are expected to differ depending on the weather location (i.e., dry Vs humid) and façade orientation. In addition, the winter performance of the system was not assessed, and its gross yearly benefits were never quantified. More importantly, the conducted case study considered constant supplies of 0.2 m^3/h of water and 54 m^3/h of air to the system subcomponents, which may not be ideal for optimal performance. This study proposes a control algorithm between the system subcomponents for optimal performance, which is expected to mitigate differences in system performance between dry versus humid conditions, and also conducts yearly simulations to investigate the winter and summer outcomes of the system installation on offices with four different orientations in Doha and Riyadh. These two locations represent countries suffering from hot dry and hot humid weather conditions almost throughout the year.

2.4. Control algorithm

As previously mentioned, the case study carried out previously considered no control algorithm between the system subcomponents, but simply constant flow rates of water and air. However, supplying constant flow rates may not yield optimal system performance.

In the evaporative cooler, sensible and latent heat exchanges take place. According to literature [25], and as per the developed model [23], it was noticed that latent heat exchange cooling effect is more significant than that of the sensible heat. However, when hot outdoor air is very humid (i.e., humidity ratio is higher than the saturated humidity of air at water temperature), no latent heat exchange occurs, and sensible exchange solely dominates. Hence, in countries that suffer from humid weather conditions throughout the year, designing long evaporative cooler along the space floor, for maximum sensible cooling, becomes advantageous.

In the long evaporative cooler, the air velocity is critical. On one hand, high air velocity intensifies the convection heat and mass transfer coefficients, which yields higher cooling efficiency. Yet, this high velocity lowers the cooling time in the evaporative cooler before air reaches its outlet. On the other hand, low air velocity decreases the cooling efficiency but increases the cooling time. Thus, the speed of air supplied to the evaporative becomes a trade-off between cooling efficiency and cooling time. The same applies to the evaporative-cooled façade where the trade-off is between the heat extraction capacity and time.

A thorough investigation has been carried out for that purpose across three different dimensions: 1- conducting several experimentations at different air speeds to ensure the validity of the model under different conditions, 2- sensitivity analysis on the air speed in the model for conditions that are not practically achievable experimentally, and 3- scenario analysis assuming different system physical dimensions, and indoor & outdoor conditions After critical investigation, the air flux inside the evaporative cooler and evaporatively-cooled façade turned out to have a dominant effect over both heat and mass exchanges combined. Consequently, supplying air at low velocities was found desirable. Nonetheless, within this low-speed band, an incremental change

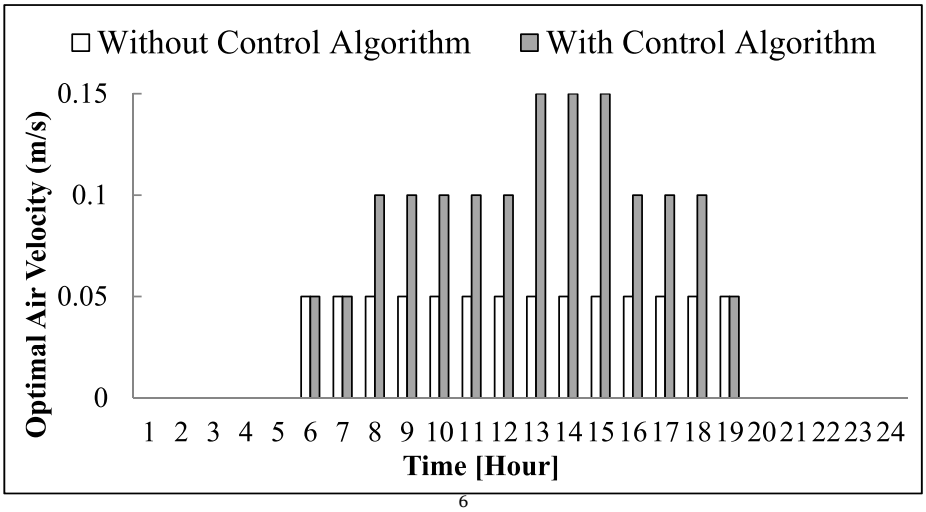

Fig. 6. Optimal air velocity for the system with and without the control algorithm during one representative (July 15th) in Doha, Qatar.

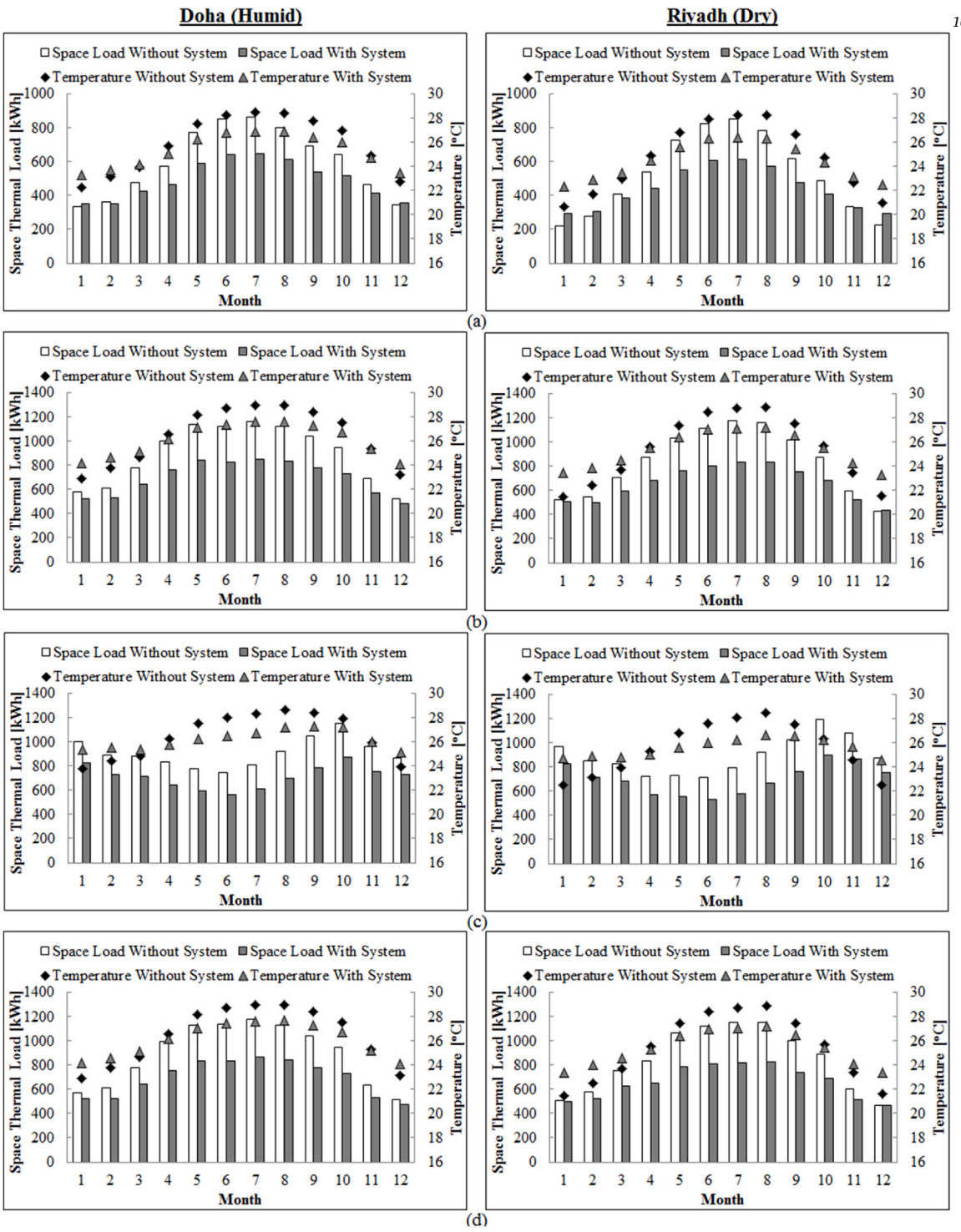

Fig. 7. The monthly thermal performance of the spaces oriented towards the (a) North, (b) East, (c) South and (d) West in Doha (humid) and Riyadh (dry).

in the air velocity may sometimes have a positive effect on cooling. Therefore, the optimal performance is the one that maximizes the heat exchange efficiency by intensifying the heat and mass transfers at the lowest possible cooling time.

For the optimal system performance, a measurable and quantifiable criterion had to be defined. The criterion selected for the air speed inside the system channel is the one that results in the lowest possible façade surface temperature. Regardless of the outdoor driving weather conditions, the least façade temperature is always desirable; in the summer, it provides maximum reduction in the space energy demands whereas in the winter, it yields maximum heat loss in a space whose load is still positive [18]. Hence, the following control algorithm is proposed.

As shown in Fig. 4, the algorithm first takes the space and system dimensions and properties as inputs to the model, and initializes all surface temperatures arbitrarily. As outdoor driving conditions are fed into the model, namely the solar radiation, dry-bulb temperature and relative humidity, the algorithm checks for the presence of solar radiation at each time-step (hourly time-steps were taken during which parameters are assumed to be constant). If present, the algorithm runs the PVT

Table 5
Annual energy savings in Doha (humid) and Riyadh (dry) for offices in four different orientations.

Doha (Humid)				
Total Energy Demand	North	East	South	West
Without System (kWh/m^2)	239.3	356.8	362.8	356.0
With System & Control Algorithm (kWh/m^2)	197.2	279.2	284.4	278.7
Total Energy Savings (%)	17.6%	21.8%	21.6%	21.7%
Incremental Energy Savings Due to Control Algorithm (%)	1.8%	2.2%	2.2%	2.2%
Riyadh (Dry)				
Without System (kWh/m^2)	210.4	335.2	357.2	338.0
With System & Control Algorithm (kWh/m^2)	176.2	263.9	280.5	265.2
Total Energy Savings (%)	16.2%	21.3%	21.5%	21.6%
Incremental Energy Savings Due to Control Algorithm (%)	1.6%	2.1%	2.2%	2.2%

model and outputs the water temperature at the outlet of the panel. Then, the evaporative cooler, which discretizes the heat and mass transfer balance equations into algebraic equations using the implicit numerical scheme, uses the water temperature from the panel outlet to find the air temperature and humidity distributions along this section based on a 0.05 m/s air velocity. Later, the algorithm reaches the evaporatively-cooled façade section and uses the adjacent space model to calculate the new temperature distributions along the outer glass, induced air, façade, and all indoor space walls. Based on the new temperature calculations, the algorithm iterates assuming the same initial air velocity until the relative error between any two iterations is less than 10^{-3} at any discretized node. Having found the proper façade surface temperature at the designated time-step, the algorithm proceeds by repeating all the aforementioned steps at different air velocities ranging between 0.05 m/s and 1.0 m/s, with increments of 0.05 m/s. Once the façade temperature at each air velocity is found for one specific time-step, the optimal speed is selected as the one that leads to the least façade surface temperature. Subsequently, the algorithm proceeds to the next time-step where the entire process is repeated until the optimal air speeds are found at all sunlit hours of the day. Note that during the hours when solar radiation is not present, the control algorithm skips the PVT and evaporative cooler models, and proceeds from the evaporatively-cooled model assuming no airflow in the channel.

After all optimal walls and façade temperatures are found at all time-steps, the space load and cumulative daily thermal energy demand are calculated for results assessment. Lastly, note that after implementing the control algorithm, and during the annual simulations, inputs from one day are used for next day, and simulations were run over many cycles to eliminate the effect of initial conditions.

2.5. Weather data

One major problem behind the failure of many solar-driven technologies is the inappropriate prediction, or often the overestimation, of the driving weather conditions. In fact, most applications rely either on outdated data, which may not be accurate currently, or on theoretical model, which may be imprecise compared to the real situations [21,31,32]. Moreover, for the proper implementation of any solar-driven technology, including the evaporatively-cooled façade system, accurate data for all outdoor driving parameters is crucial, especially that most failures have been historically caused by the overestimation of this data.

One source of weather data is the EnergyPlus Weather (.epw), which averages different meteorological statistics (e.g., temperature, humidity, radiation) over a finite number of years [33]. Since no data examination could be done on this weather file (e.g., sensing control, quality assurance, or data cleaning), and to ensure that standard approaches were used for typical meteorological year, data validation was deemed necessary. For this reason, and to ensure that data extracted from this source is representative, at least those used in and directly relevant to this study, hourly and monthly averages for Doha, Qatar, were compared with those measured experimentally at the meteorological site of the Zero Emission Laboratory at Qatar University, continuously over the year of 2016. Details of the prepared instrumentation and maintenance, data gathering, and analysis are documented by A. Al Touma & D. Ouahrani [21]. Data validation for temperature, relative humidity, and global horizontal and vertical irradiances (on south surface) was carried out.

The maximum discrepancy in monthly averages between EnergyPlus weather file and experimental recordings was less than 2.0 °C in October for temperature and 9% in April for relative humidity. Similarly, the largest difference was 1.6 kWh/m^2 and 1.5 kWh/m^2 for daily global horizontal irradiance in December and global vertical irradiance (in south orientation), respectively. A closer look at the hourly data, especially during typical representative days, shows that both trends are comparable with statistically significant correlations. Hence, it was concluded that EnergyPlus (epw) parameters do in fact represent current weather conditions, and consequently can be reliably used for the purpose of this study. The weather data used for Doha (Qatar) and Riyadh (Saudi Arabia) is shown in Fig. 5.

As seen in Fig. 5(a), the average dry-bulb temperature per day in Doha ranges between 18.3 °C in January and 35.7 °C in August, whereas the average relative humidity per day varies between 37% in May and 66% in December. On the other hand, global horizontal irradiance ranges between 3.3 kWh/m^2 in December and 7.6 kWh/m^2 in May. Similarly, Riyadh shows an average monthly temperature that ranges between 14.0 °C in January and 36.4 °C in August, and a relative humidity between 8% in July and 57% in December. Global horizontal irradiance varies between monthly averages of 4.1 kWh/m^2 and 8.0 kWh/m^2, as exhibited in Fig. 5(b). It is of interest to highlight the similarities of the two weathers in temperature and solar radiation, as exhibited by root mean square errors (RMSE) of less than 2.8 °C in temperature and 0.7 kWh/m^2 in horizontal irradiance, and the substantial difference in relative humidity with a RMSE of 31%, which is expected to practically isolate the effect of that parameter to draw scientific conclusions on the capability of the control algorithm to overcome that difference. Also, and as anticipated based on both cities' longitude, it is expected that solar radiation striking vertical surfaces in south orientations are the most prominent, whereas north-orientations are typically least hit and affected by this parameter.

2.6. A case study

From the validated simulation, the space model was adjusted to mimic real-life conditions using the developed control algorithm applied on the evaporatively-cooled façade. An office space, of 6 m × 5 m dimensions and a height of 2.8 m, was considered. The office has one fully glazed façade, with dimensions of 6 m × 2.8 m, facing one orientation (e.g., north, east, south, or west), whereas the rest of the walls, floor, and ceiling are all assumed to be internal and adjacent to other conditioned spaces.

The space envelope was selected from popular actual construction practices followed in the Arabian Gulf [34,35]. Moreover, the construction envelope abides by the regional standards set for buildings in harshly hot climates [35]. The details of the space thermal envelope are provided in Table 2. As for the evaporatively-cooled façade system (i.e., PVT, evaporative cooler, and glazed section), its technical specifications are also summarized in Table 2. Note that the outer glass is just a 6 mm clear glass layer of 0.88 and 0.77 visible and solar transmissivities, which is expected not to impact the visual eyesight of the space occupants.

The space was set to have an indoor temperature of 24 °C. Lastly, and to mimic real conditions, the space is set to have some internal loads, as detailed in Table 3. All internal loads are activated during the

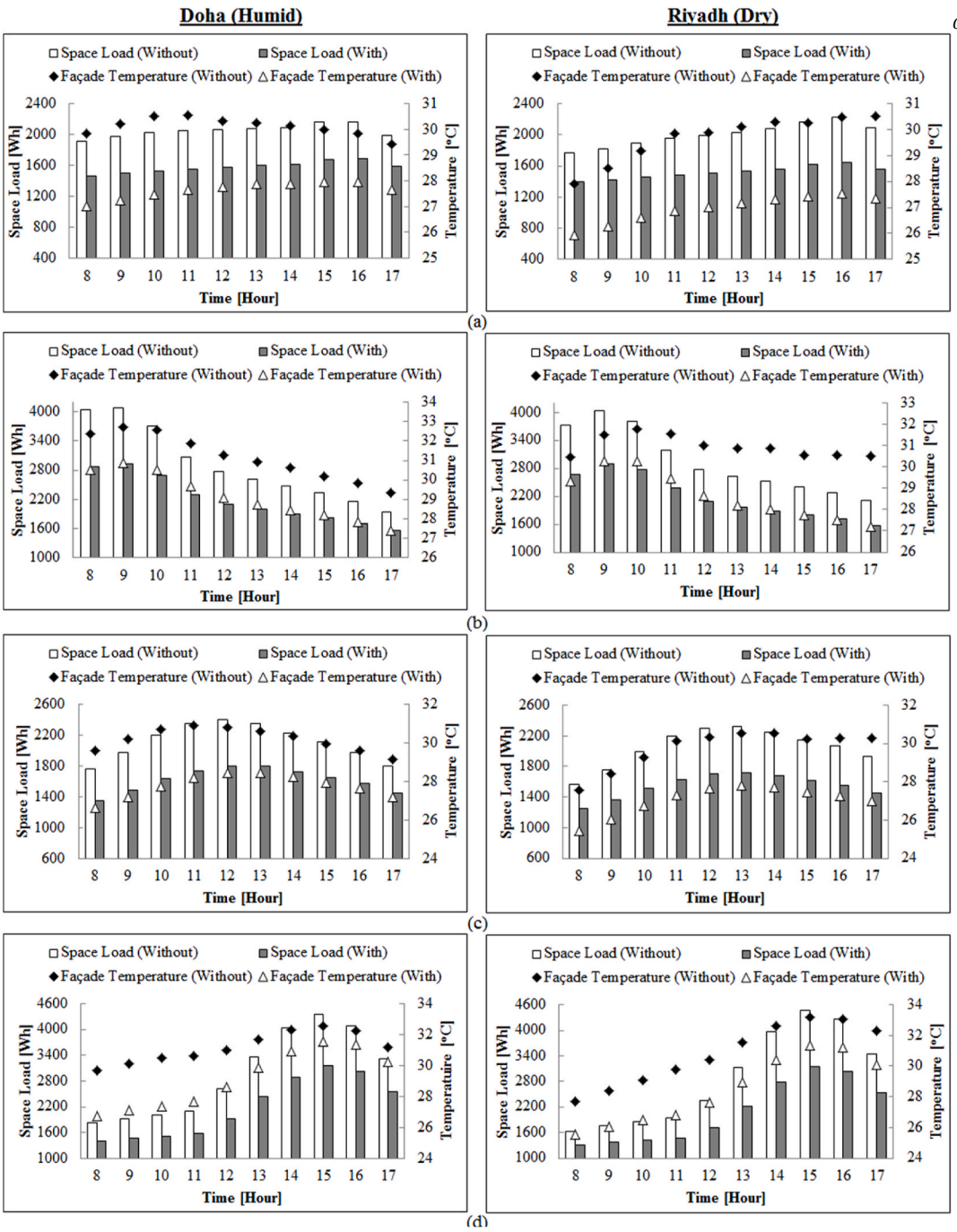

Fig. 8. The hourly thermal performance of the spaces oriented towards the (a) North, (b) East, (c) South and (d) West during one summer representative day in Doha (humid) and Riyadh (dry).

normal working hours of the day (weekdays only) from 8AM (9 h) to 6PM (19 h) [20].

3. Results and discussion

3.1. The application of control algorithm

To assess its benefits, simulations on the system were carried out with and without the control algorithm, under exactly the same set of inputs and driving conditions, and were compared to a base-case office space without the system installed on the façade. These simulations were conducted for Doha on July 15th; a summer representative day where the temperature varied between 32.9 °C and 40.0 °C, and the relative humidity ranged between 42.3% and 73.9%. Results of the façade daily heat gain and hourly optimal air velocity are shown in Table 4 and Fig. 6.

As seen in Table 4, the reduction in the façade daily thermal heat gain is intensified from 33.5% to 38.3% when the control algorithm is integrated to the system. This is because supplying air at a constant speed turned out to be suboptimal for the system performance. Although low airspeeds (i.e., 0.05 m/s) are preferable for maximum air cooling inside the evaporative cooler, incremental changes in the air velocity inside the channel during certain hours were found favorable in obtaining the least possible façade hourly surface temperatures, especially during the hours when heat gain is typically large (e.g., 10–16 h). These incremental changes, from 0.05 m/s to 0.1 m/s and 0.15 m/s be-

Table 6
Savings in the façade heat gain and space total thermal energy demand during one summer representative day in Doha (humid) and Riyadh (dry) for offices in four orientations.

Doha (Humid)				
	North	East	South	West
Energy Demand Without System (kWh)	27.9	39.7	27.7	40.0
Energy Demand With System & Control Algorithm (kWh)	20.4	28.6	20.3	28.9
Total Savings in Energy Demand (%)	26.8%	28.1%	26.7%	27.9%
Incremental Total Savings Due to Control Algorithm (%)	2.7%	2.8%	2.7%	2.8%
Savings in Façade Heat Gain (%)	47.6%	37.5%	47.8%	36.4%
Riyadh (Dry)				
Energy Demand Without System (kWh)	26.7	38.7	26.5	38.6
Energy Demand With System & Control Algorithm (kWh)	19.3	27.6	19.2	27.5
Total Savings in Energy Demand (%)	27.6%	28.7%	27.6%	28.6%
Incremental Total Savings Due to Control Algorithm (%)	2.8%	2.9%	2.8%	2.9%
Savings in Façade Heat Gain (%)	53.2%	41.0%	53.2%	40.3%

tween 8 and 16 h, as seen in Fig. 6, enhanced the performance of the system, and consequently decreased the space heat gains even further. Hence, the control algorithm implemented and integrated on the evaporatively-cooled façade system turned out to be beneficial in providing additional savings of 2.7% to the space thermal loads during this day. Note that the increase in the energy consumption of the fan is expected to have a marginal effect on the total space electricity consumption and bill, considering its relatively small size (e.g., 50 W Elekta [23]). For the day under consideration, for instance, the fan energy consumption went up from 0.10 kWh to 0.19 kWh throughout the entire day, and a PVT of just 1.56 m^2 in size with a small storage battery were deemed satisfactory to meet this demand (refer to Table 2).

3.2. Monthly and yearly performances

As the annual performance of the evaporatively-cooled façade system was never evaluated, the simulation model was adjusted to feed the hourly weather data (e.g., temperature, relative humidity, global horizontal irradiance …) throughout the year for the office space considering four different orientations: north, east, south, and west. The simulations were also carried out for both Doha (Qatar) and Riyadh (Saudi Arabia), mimicking cities with harshly humid & dry weather conditions, respectively. Note that the space thermal load was calculated as the summation of the individual hourly loads of the façade and walls, including the floor and ceiling, whereas the energy demand was the corresponding accumulation for daily, monthly, and annual performances. Results are shown in Fig. 7 and Table 5. Note that the incremental energy savings due to the integration of the control algorithm are calculated as the additional reductions seen after implementing the control algorithm, in comparison with the case when the system is installed without any control over its components.

As seen in Fig. 7, the system installation on the spaces had a positive effect on the façade by decreasing its temperature in all four orientations, especially during the summer, with some slight adverse effect during the winter. However, the magnitude of the decrease was different depending on the façade orientation:

- Due to the countries' latitudes, north orientations in Qatar & Saudi Arabia are typically façades struck by least amount of solar radiation. When installed, the façade average temperature decreased by up to 1.4 °C and 1.8 °C during the hot month of August in Doha and Riyadh, respectively. This decrease led to a reduction of 38.2% and 18.4% in the monthly façade and total space heat gains in Doha respectively, and of 50.6% and 21.6% in Riyadh. Since the latter is a city exhibiting dryer weather conditions, the impact of the system installation was larger. However, the system performed poorly, or sometimes adversely, in the wintertime. During winter, outdoor temperature is expected to be lower than indoor temperature, hence reversing the effect of the system, especially when hit by minimal solar radiation. Nonetheless, this adverse effect of the system during winter is not expected to jeopardize the indoor conditions but, on the contrary, enhance indoor thermal comfort and radiation symmetry (i.e., less radiation asymmetry). These impacts will need to be investigated by the authors later in a separate study. Throughout the year, the system managed to decrease the space total energy demands by 17.6% and 16.2% in Doha and Riyadh, respectively.
- In east and west orientation, the system performed advantageously almost throughout the year. It managed to decrease the monthly average temperature by up to 1.1 °C in Doha and 1.4 °C in Riyadh. For the same humidity reasons, the application of the system in Riyadh outperformed Doha. It is of interest to note that, although the façade temperature barely increased during the winter, the system still performed favorably in terms of space load. This is because the combined effect of less radiation transmission into the space and less internal walls temperature outweighed the minimal increase in façade temperature. Note that east and west orientations are hit by considerable solar radiation even during the winter, which allows the system to still perform well. In July, its application managed to reduce the monthly façade heat gain and space total heat gain by up to 27.5% and 17.7% in Doha, and by up to 36.0% and 19.9% in Riyadh, respectively. Throughout the year, the system integrated with the control algorithm decreased the space total energy demands by 21.8% in Doha and 21.6% in Riyadh.
- The application of the system on south-oriented façades managed to reduce their average monthly temperature by 1.5 °C in Qatar and 1.9 °C in Saudi Arabia. The system installation on the façades that are most struck by solar radiation managed to decrease the monthly façade heat gain by 42.1% in Qatar and 51.3% in Riyadh. Ultimately, this led to reductions in the total monthly heat gain in July of 18.7% and 21.8%, and annual reductions of 21.6% and 21.5% in Doha and Riyadh respectively, as shown in Table 5.

As exhibited in Fig. 7and Table 5, it is of interest to highlight the parity in the system performance between the dry and humid weather conditions. This parity, which is quantified in smaller differences than previously shown in other studies [23], can only be attributed to the application of the control algorithm that optimizes parameters inside the evaporatively-cooled façade system to yield the best possible performance. Also, it important to note that the control algorithm alone managed to contribute into to space total energy savings by increments of between 1.6% and 2.2% in both cities, above those resulting from the simple installation of the system itself.

3.3. Summer performance

To better assess the impact of system installation on the space, integrated with the developed control algorithm, summer and winter representative days analyses were carried out separately. For the summer days, individual simulations were conducted on July 21st, representing the harsh summer conditions in the Arabian Gulf. The façade temperature and space total load for spaces with and without the system installed in four different orientations are shown in Fig. 8, whereas overall daily energy savings are tabulated in Table 6:

- In north orientations, and when the system is not installed, the façade surface temperature is of symmetrical shape, around 11 h in Doha with a peak value of 30.5 °C, and around 16 h in Riyadh with a peak value of 30.6 °C. The installation of the evaporatively-cooled

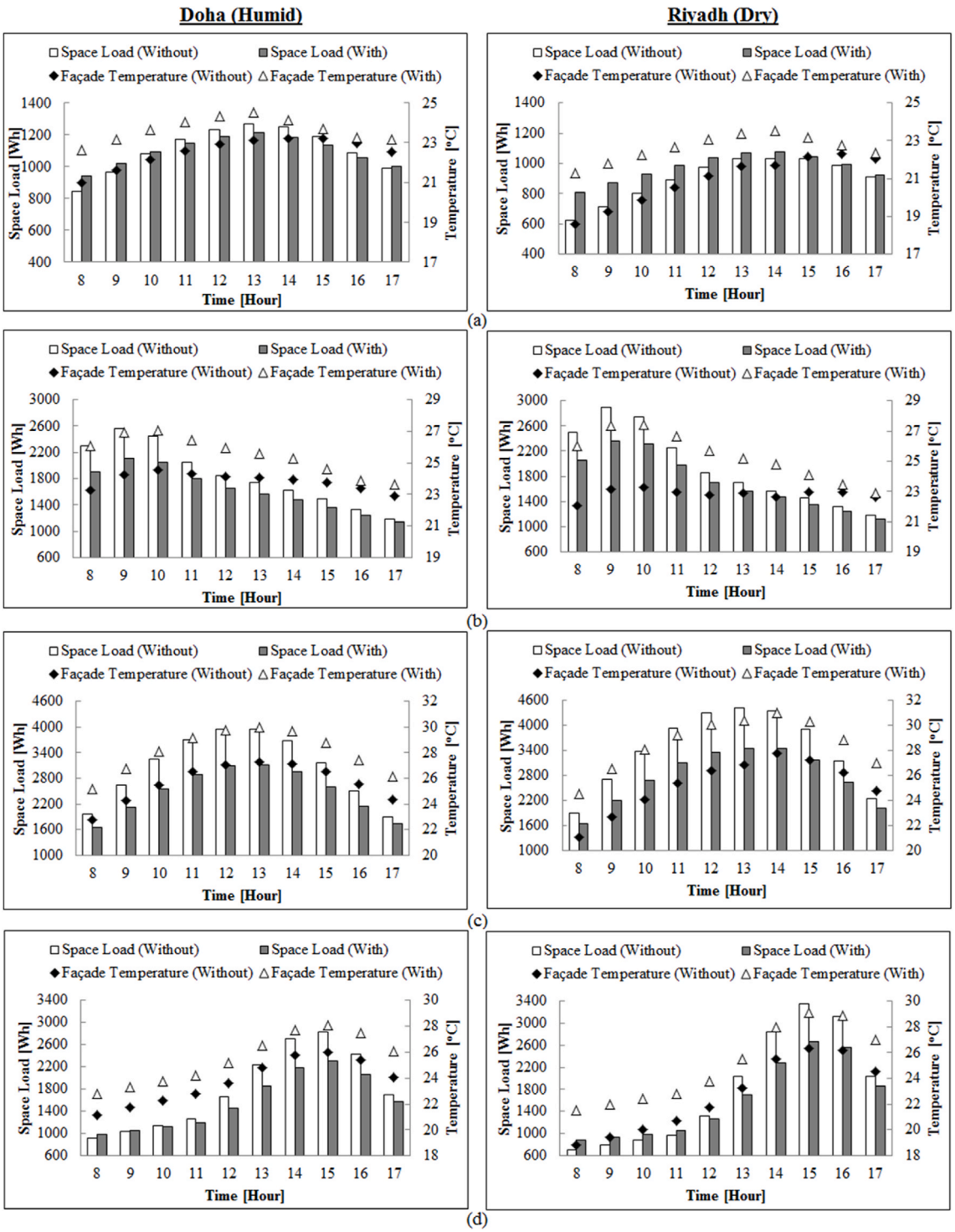

Fig. 9. The hourly thermal performance of the space oriented towards the (a) North, (b) East, (c) South and (d) West during one winter representative day in Doha (humid) and Riyadh (dry).

façade system on the space reduced its façade peak temperature to 27.8 °C for both cities. This decrease has cut the façade heat gain almost by half, and the space total daily energy demand by 26.8% and 27.6% in Doha and Riyadh, respectively (Table 6). Despite the significant difference in weather conditions, especially during the summer (i.e., humid Vs dry), the spaces performed quite similarly when the system was installed.

- Spaces directed towards the east, with no system, have peak façade temperature values in the early hours of the day of 32.7 °C (at 9 h) in Doha and of 31.8 °C (at 10 h) in Riyadh. After the system was applied, façade temperature reduced significantly throughout the day, with peak values of 31.6 °C and 30.8 °C in Doha and Riyadh respectively, ultimately saving 28.1% and 28.7% of the spaces total daily heat gains (Table 6). Spaces directed towards the west have similar performances, except that peak values, and corresponding reductions, are shifted to the later hours of the day at 15 h in Doha and Riyadh. Similar total daily savings of 27.9% and 28.6% are found.

Table 7
Reductions in the façade heat loss and space total thermal energy demand during one winter representative day in Doha (humid) and Riyadh (dry) for offices in four orientations.

Doha (Humid)				
	North	East	South	West
Energy Demand Without System (kWh)	9.3	18.9	33.1	18.6
Energy Demand With System & Control Algorithm (kWh)	11.5	20.0	32.6	19.9
Total Savings in Energy Demand (%)	−24.7%	−5.7%	1.6%	−7.2%
Incremental Total Savings Due to Control Algorithm (%)	−2.5%	−0.6%	0.2%	−0.7%
Reductions in Façade Heat Loss (%)	67.3%	117.7%	381.1%	124.2%
Riyadh (Dry)				
Energy Demand Without System (kWh)	5.0	18.1	35.9	17.8
Energy Demand With System & Control Algorithm (kWh)	8.8	20.0	35.8	20.2
Total Savings in Energy Demand (%)	−76.1%	−10.8%	0.1%	−13.4%
Incremental Total Savings Due to Control Algorithm (%)	−7.6%	−1.1%	0.0%	−1.3%
Reductions in Façade Heat Loss (%)	56.0%	84.9%	190.6%	92.6%

- In south orientations, which are the most troubling during summertime, the façade temperature is of symmetrical shape, with peak value reaching 30.9 °C and 30.6 °C in Doha and Riyadh, respectively, without the system. After the installation of the evaporatively-cooled façade system, the façade exhibited a significant reduction in its temperature, whose peak value reached 28.8 °C and 28.0 °C in the two cities. This significant change in the façade temperature managed to halve the façade daily heat gain, which resulted in savings of 26.7% and 27.6% in Doha and Riyadh, respectively (Table 6).

Moreover, the impact of the control algorithm alone, isolated from the system itself, enhanced the space total energy savings by up to 2.9%. It is of interest to mention that, despite the considerable humidity differences between Doha and Riyadh during summertime (a monthly relative humidity average of 47% in Doha versus 8% in Riyadh; refer to Fig. 5), and considering the drastic limitation in system performance when applied without any optimization to its internal parameters (total annual savings of 14.5% only in Qatar [23]), the system now performed quite similarly when applied in both dry and humid conditions during the summertime, when integrated with the control algorithm, irrespective of the façade orientation. This similarity can only be attributed to the control algorithm that optimized the system in general, and of the evaporative cooler cooling effect and glazing section heat extraction effect in specific.

3.4. Winter performance

In the winter, the outdoor temperature is expected to be lower than the indoor set-point temperature (i.e., 24 °C). However, considering the space internal loads and space orientation, energy demands may still be positive. If fact, it will most likely be positive when the space is oriented towards the east, south, and west (i.e., struck by considerable solar radiation), and negative otherwise (i.e., when hit by least solar radiation in north orientation). Consequently, the application of the system in the winter is more complex; on one hand it reduces solar radiation transmission into the space, which brings the heat gain down, and on the other hand, it reduces heat loss form the space to the outer environment, which brings the space heat gain up. Hence, the installation of the system is a trade-off between these two effects. It is important to mention that, in this study, the visual comfort of the space occupants was assumed to be of upmost important and will not be compromised; hence, an outer glass of high solar and visual transmissivities was selected for the system (refer to Table 2). Thus, the impact of the reduced heat loss from the space outwards is expected to outweigh any reduction in solar radiation penetration into the space in some orientations, and vice versa in some others. For further analysis, simulations were carried out for January 21st, representing typical winter day in the Arabian Gulf. Results are shown in Fig. 9 and Table 7.

- In north-oriented spaces, the façade temperature reached a maximum of 23.2 °C in Doha and 22.3 °C in Riyadh when the system was not installed. When installed, the façade temperature value increased to 24.8 °C and 23.6 °C, respectively. In these cases, heat losses from the space outwards decreased (i.e., heat gains increased) as reflected in Table 7, and outweighed the humble reductions in solar radiation penetration, thus leading to an increase in the space daily thermal energy demand by 24.7% (i.e., 2.2 kWh) in Doha and 76.1% (i.e., 3.8 kWh) in Riyadh.
- In east-oriented spaces, the peak façade temperature went up from 24.5 °C at 10 h to 27.7 °C when the system is installed in Doha, and from 23.3 °C to 28.0 °C in Riyadh. Similarly, the application of the system on west-oriented spaces brought the façade temperature up from 26.0 °C at 15 h to 28.7 °C in Doha, and from 26.3 °C to 29.5 °C in Riyadh. These changes have increased the space hourly load, outweighed any reductions in solar radiation transmission into the space, and brought the space daily thermal energy demand up slightly by 7.2% (i.e., 1.3 kWh) in Doha and 13.4% (i.e., 2.4 kWh) in Riyadh.
- For south-oriented offices, the application of the system increased the façade peak temperature from 27.3 °C at 13 h to 30.9 °C in Doha, and from 27.8 °C at 14 h to 31.5 °C in Riyadh. However, and since these surfaces are hit by significant solar radiation during the winter, this increase in façade temperature was less than the reduction effect of the solar radiation transmission, and the system still performed advantageously. This aggregate impact yielded a minimal decrease in the space daily total thermal energy demand of less than 1.6% and 0.1% in Doha and Riyadh, respectively.

As explained, and irrespective of the space orientation, the installation of the system increased the thermal resistance of the façade, and consequently reduced the heat loss from the space façade to the outer environment. However, the magnitude of the increased heat gains outweighed any reductions in solar radiation penetration into the space in north, east, and west surfaces. For this reason, these surfaces reduced energy savings by up to 7.6% due to the control algorithm during wintertime. On the other hand, south surfaces proved a barely positive system performance even during the winter.

It is of interest to mention that the adverse performance of the system during the winter does not render it undesirable. This is because slight increases in the façade surface temperature are sometimes expected to enhance the space thermal comfort for the indoor occupants and reduce the corresponding radiation asymmetry. However, these presumptions would need to be further investigated by the authors in a separate future study to assess whether the proposed control algorithm should be activated or turned off during the winter depending on the façade orientation. Lastly, the similarity in outcomes for Doha and Riyadh is again the result of optimal system performance caused by the integration of the developed control algorithm.

4. Conclusions

In this study, the previously developed evaporatively-cooled façade system, when applied on office spaces, was further investigated for optimal performance. A control algorithm was developed to overcome the limitation of the system in general, and the evaporative cooler in specific, when installed in humid locations, and consequently yield maximum possible energy savings. The control algorithm optimizes the entrained airspeed inside the system, as per the outdoor conditions, to

generate the lowest possible façade surface temperature. The integration of the control algorithm on the system managed to further increase the reductions in façade heat gain from 33.5% to 38.3%, in comparison with a normal space with no system at all, and add an additional 2.7% savings to the space daily energy demands. More importantly, this control algorithm successfully managed to reduce the differences in system performance in dry versus humid locations.

Annual simulations were then carried out for offices in four different orientations (i.e., north, east, south, and west) and located in both Doha (Qatar) and Riyadh (Saudi Arabia), representing locations with harshly hot humid and dry weather conditions, respectively.

- During the summer, the system has a considerable impact in reducing the façade surface temperature, subsequently leading to savings in the space thermal energy demand by up to 28.7%
- During the winter, the application of the system increased the façade surface temperature. This change, however, was still advantageous in south orientation, but slightly adverse in north, east, and west-oriented spaces. Nonetheless, since thermal loads for spaces in the Arabian Gulf are already minimal during wintertime, such increases are expected to have marginal impact on energy bills, but a relatively larger, possibly positive, effect on the indoor occupants' thermal comfort. This hypothesis is yet to be investigated by the authors in a future study
- Throughout the year, the system, integrated with the control algorithm, has a significant positive impact the space thermal energy demands. Its installation on spaces in different orientations led to total aggregate annual savings of between 16.2% and 21.8%, depending on the space orientation

The incremental costs that must be incurred to set up the system are around USD 1200; considering the corresponding reductions in total energy demand, the benefits cover monetary savings of ~USD 60–80 in the Arabian Gulf, hence a payback period of 15–20 months.

Lastly, the future work of the authors includes the quantification and optimization of the amount of water used by the system, a detailed assessment of system impact on the thermal comfort of the occupants during the winter, as well as the integration and simulation of such a system into the wider concepts of smart buildings (i.e., fully-glazed buildings with numerous offices across all directions) in the Arabian Gulf.

Declaration of competing interest

The authors declare that they have no known competing financial interests or personal relationships that could have appeared to influence the work reported in this paper.

Acknowledgment

The financial and in-kind support of Qatar University in setting up the Zero Emission Laboratoryis greatly acknowledged.

References

[1] B. Petroleum, BP Statistical Review of World Energy, 2017.
[2] S. Said, M. Habib, M. Iqbal, Database for building energy prediction in Saudi Arabia, Energy Convers. Manag. 44 (2003) 191–201.
[3] Q.G. Electricity, Water Corporation KAHRAMAA, Statistical Report, 2015, p. 2015.
[4] A. Al Touma, N. Ghaddar, K. Ghali, Energy savings of windows with shutters in hot and humid climates, Proceedings of the 2nd ASHRAE International Conference on Efficient Building Design: Materials and HVAC Equipment Technologies, ICEBD-MET: 2016–21201, Beirut, Lebanon, 2016, pp. 22–23 September, 2016.
[5] A. Al Touma, D. Ouahrani, Experimental analysis of double and triple glazed façades with different shading devices in Qatar, Sustainable and Renewable Energy Engineering (ICSREE), 2017 2nd International Conference, IEEE, 2017, May, pp. 38–41.
[6] K.J. Kontoleon, Dynamic thermal circuit modelling with distribution of internal solar radiation on varying façade orientations, Energy Build. 47 (2012) 139–150.
[7] K. Tsikaloudaki, K. Laskos, T. Theodosiou, D. Bikas, Assessing cooling energy performance of windows for office buildings in the Mediterranean zone, Energy Build. 49 (2012) 192–199.
[8] K. Tsikaloudaki, T. Theodosiou, K. Laskos, D. Bikas, Assessing cooling energy performance of windows for residential buildings in the Mediterranean zone, Energy Convers. Manag. 64 (2012) 335–343.
[9] N. DeForest, A. Shehabi, G. Garcia, J. Greenblatt, E. Masanet, E.S. Lee, D.J. Milliron, Regional performance targets for transparent near-infrared switching electrochromic window glazings, Build. Environ. 61 (2013) 160–168.
[10] H. Ye, L. Long, H. Zhang, Y. Gao, The energy saving index and the performance evaluation of thermochromic windows in passive buildings, Renew. Energy 66 (2014) 215–221.
[11] M. Arıcı, H. Karabay, M. Kan, Flow and heat transfer in double, triple and quadruple pane windows, Energy Build. 86 (2015) 394–402.
[12] T.T. Chow, Z. Lin, K.F. Fong, L.S. Chan, M.M. He, Thermal performance of natural airflow window in subtropical and temperate climate zones–a comparative study, Energy Convers. Manag. 50 (8) (2009) 1884–1890.
[13] J. Wei, J. Zhao, Q. Chen, Energy performance of a dual airflow window under different climates, Energy Build. 42 (1) (2010) 111–122.
[14] S.F. Larsen, L. Rengifo, C. Filippín, Double skin glazed façades in sunny Mediterranean climates, Energy Build. 102 (2015) 18–31.
[15] K. Zhong, S. Li, G. Sun, S. Li, X. Zhang, Simulation study on dynamic heat transfer performance of PCM-filled glass window with different thermophysical parameters of phase change material, Energy Build. 106 (2015) 87–95.
[16] C. Li, J. Tan, T.T. Chow, Z. Qiu, Experimental and theoretical study on the effect of window films on building energy consumption, Energy Build. 102 (2015) 129–138.
[17] D. Ouahrani, A. Al Touma, Selection of slat separation-to-width ratio of brise-soleil shading considering energy savings, CO_2 emissions and visual comfort–A case study in Qatar, Energy Build. (2017).
[18] A. Al Touma, D. Ouahrani, Shading and day-lighting controls energy savings in offices with fully-Glazed facades in hot climates, Energy Build. 151 (2017) 263–274.
[19] M.H. Oh, K.H. Lee, J.H. Yoon, Automated control strategies of inside slat-type blind considering visual comfort and building energy performance, Energy Build. 55 (2012) 728–737.
[20] A. Al Touma, K. Ghali, N. Ghaddar, N. Ismail, Solar chimney integrated with passive evaporative cooler applied on glazing surfaces, Energy 115 (2016) 169–179.
[21] A. Al Touma, D. Ouahrani, Performance assessment of evaporatively-cooled window driven by solar chimney in hot and humid climates, Sol. Energy 169 (2018) 187–195.
[22] W.A. Hweij, A. Al Touma, K. Ghali, N. Ghaddar, Evaporatively-cooled window driven by solar chimney to improve energy efficiency and thermal comfort in dry desert climate, Energy Build. 139 (2017) 755–761.
[23] A. Al Touma, D. Ouahrani, Evaporatively-cooled façade integrated with photovoltaic thermal panel applied in hot and humid climates, Energy 172 (2019) 409–422.
[24] M. Herrando, C.N. Markides, K. Hellgardt, A UK-based assessment of hybrid PV and solar-thermal systems for domestic heating and power: system performance, Appl. Energy 122 (2014) 288–309.
[25] M.H. Kim, D.S. Jeong, J.W. Jeong, Practical thermal performance correlations for a wet-coil indirect evaporative cooler, Energy Build. 96 (2015) 285–298.
[26] A. Hagishima, J. Tanimoto, Field measurements for estimating the convective heat transfer coefficient at building surfaces, Build. Environ. 38 (7) (2003) 873–881.
[27] M.H. Vorre, R.L. Jensen, J. Le Dreau, Radiation exchange between persons and surfaces for building energy simulations, Energy Build. 101 (2015) 110–121.
[28] J.A. Duffie, W.A. Beckman, Solar Engineering of Thermal Processes, 1980.
[29] T.L. Bergman, F.P. Incropera, Fundamentals of Heat and Mass Transfer, John Wiley & Sons, 2011.
[30] B. Yassine, K. Ghali, N. Ghaddar, I. Srour, G. Chehab, A numerical modeling approach to evaluate energy-efficient mechanical ventilation strategies, Energy Build. 55 (2012) 618–630.
[31] T. Pan, S. Wu, E. Dai, Y. Liu, Estimating the daily global solar radiation spatial distribution from diurnal temperature ranges over the Tibetan Plateau in China, Appl. Energy 107 (2013) 384–393.
[32] J. Almorox, C. Hontoria, M. Benito, Models for obtaining daily global solar radiation with measured air temperature data in Madrid (Spain), Appl. Energy 88 (5) (2011) 1703–1709.
[33] EnergyPlus documentation, https://energyplus.net/documentation.
[34] N. Ayoub, F. Musharavati, S. Pokharel, H.A. Gabbar, Energy consumption and conservation practices in Qatarda case study of a hotel building, Energy Build. 84 (2014) 55–69.
[35] The Saudi Building Code (SBC) - Section 601: Energy Conservation, 2007.
[36] ASHRAE, Standard 62.1. Ventilation for Acceptable Indoor Air Quality, 2004.
[37] Standard ASHRAE, Energy standard for buildings except low-rise residential buildings, ASHRAE/IESNA Stand 90 (1) (1999).